THERMAL LOSSES REDUCTION FOR A TROUGH COLLECTOR: PART 2 HEAT TRANSFER

Dhafeer M. H. Al-Shamkhi
Foundation of Technical Education
Technical Engineering College/Najaf
Alternative and Renewable Energy Research Unit

Wisam A. Abd Al-Wahid
Foundation of Technical Education
Technical Engineering College/Najaf
Automotive Dept.

ABSTRACT

The heat losses by convection from the collector tube of a trough collector to the ambient areanalyzed. The strategy to reduce such losses is by using a vacuum glass tube covering the collector tube. Since the maintaining of this vacuum state is difficult, beside the high cost and easily broken off the glass tube, another strategy presented in this paper. The strategy based on reducing the overall convection heat transfer by the use of guides made of metal, which effect on the process of heat transfer. The guides put in front of the collector as a half circle with different dimensions, and each one analyzed numerically by using 4.4COMSOL Multiphysics program. The analysis include the streamlines behavior, temperature distribution, and averageNusselt number. The minimum the Nusselt number obtained the best arrangement to use. The data show a decrement in heat transfer process due to that modification with different percentages.

Keywords-Thermal losses reduction; Trough collector; Combined free and forced convection; Solar energy.

تقليل الخسائر الحرارية من مجمع شمسي: الجزء الثاني انتقال الحرارة

ظافر مانع حاجم الشمخي
هيئة التعليم التقني
الكلية التقنية الهندسية/ النجف
وحدة بحوث الطاقة البديلة والمتجددة

وسام احمد عبد الواحد
هيئة التعليم التقني
الكلية التقنية الهندسية/ النجف
قسم تقنيات هندسة السيارات

الخلاصة:

في هذا البحث, تم تحليل أنتقال الحرارة بالحمل من انبوب التجميع في المجمع الشمسي. وقد وجد بأن الستراتيجية المتبعة لتقليل انتقال الحرارة هي باستخدام انبوب مفرغ من الهواء يغطي انبوب التجميع . وبما ان تكلفة هكذا انبوب هي عالية ناهيك عن صعوبة المحافظة على التفريغ بسبب التسرب أو كسر الانبوب. لذا فقد قدم هذا البحث اسلوب جديد في تقليل الخسائر يقضي بوضع مصدات هوائية على شكل نصف دائري و بمختلف الاقطار أمام انبوب التجميع وذلك للتاثير في عملية انتقال الحرارة. وقد تم استخدام برنامج COMSOL4.1 لغرض التحليل الرياضي المتبع. وقد ضم التحليل حساب خطوط الجريان وتوزيع السرع ودرجات الحرارة. وقد تم حساب عدد نسلت والذي يعتبر مقياس تقليل الخسارة بالحصول على اقل عدد نسلت. وقد أوجدت الحسابات نقصاناً في الخسائر الحرارية من انبوب التجميع بسبب هذا التعديل وبنسب مختلفة.

Nomenclatures

Symbol	Description	Units
	Thermal expansion coefficient	J/kg.K
D	Cylinder diameter	m
Dhi	Hydraulic diameter at interring	m
Dr	Diameter ratio	
F	Volume force	N/m^3
K	Thermal conductivity	W/m.K
k	Turbulent kinetic energy	m^2/s^2
L_T	Turbulence length scale	m
l_T	Turbulence intensity	m^2/s^2
Nu	Local Nusselt number	
Nua	Average Nusselt number	
Nu_{fsp}	Average Nusselt number at front	
Nu_{max}	Maximum Average Nusselt number	
Nu_{min}	Minimum Average Nusselt number	
	Pressure	N/m^2
Pr	Prandtl number	
Re_i	Reynolds number at inlet	
	Temperature	^oK
Tamb	Inlet Temperature	^oK
Trt	Receiver tube temperature	^oK
Ttw	Trough wall temperature	^oK
U	Velocity field (u,v,w)	m/s
	Horizontal velocity	m/s
	Vertical velocity	m/s
W	Aperture of the parabolic collector	m
	Horizontal coordinate	m
y	Vertical coordinate	m

Greek Symbols

Symbol	Description	Units
	Density of air	kg/m^3
	Dynamic viscosity	$N.s/m^2$
	Turbulent Dynamic viscosity	$N.s/m^2$
ε	Rate of dissipation of kinetic energy	m^2/s^2
θ	Pitch angle	degree

1. INTRODUCTION

Solar energy is an essentially inexhaustible source of energy potentially capable of meeting a significant portion of all nation's future energy needs with a minimum of adverse environmental consequences. The current industrial growth and environmental impacts show that solar energy for solar thermal power plants is the most promising of the unconventional energy sources. The future of the solar power plant development depends on a number of serious constraints, including scientific and technological problems are deals with the most common commercially available solar power plants use parabolic trough concentrators.

Parabolic trough collector (PTC) technology is one of a number of concentrated solar power (CSP) conversion methods available today. PTC technology is becoming widely used for power generation and process heat applications. The reason for the success of PTC technology, that it is the most mature and one of the least expensive solar thermal energy technologies available in the market.

Where the thermal analysis in such solar collectors studied widely to find the optimum reduction of heat losses and collector efficiency with different flows, selective coating, and operating conditions **(Christ. 2012)**. In other hand, the whole model also studied thermally by using a finite volume method to analyze the heat transfer inside the collector, and using the Monte Carlo method to analyze the radiation heat transfer outside the collector **(Cheng. 2010)**. In addition for the previous works, the wind effect on the trough was taken in mind **(Kalogirou. 2012,Hachicha . 2012, andCheng. 2012)**, where the measurements of wind load are tabulated **(Kalogirou. 2012**). During this, the reduction of heat losses from the collectors took a great attention in order to reduce these losses **(Naeeni. 2007).**These losses mainly shown as a convection heat transfer to the ambient **(Al-Ansary. 2011)**, which is a function of pitch angle and trough orientation. The best strategy to reduce these losses is to use the vacuum glass tube in many arrangements **(Daniel. 2011)**, but the keeping of these tubes in vacuum situations is very difficult, which lead to another strategy of using insulations**(Padilla. 2011)**.

In the present work, a detailed two dimensional heat transfer analysis of a PTC presented. Three values of collector's orientations values taken as shown in figure 1 below.

Where this study focus on reducing the loss of heat from non-evacuated tube by convection to ambient for different wind speeds and by adding a half circular plate in front of the receiver as shown in figure 2. Where the effect of this plate on the average Nusselt number for the receiver tube studied for different wind speed,pitch angles, and different plate dimensions.

2. MATHEMATICAL ANALYSIS

The casual design of the parabolic trough collector is to put the receiver in the center of the trough. The receiver always covered with a glass tube with an intermediate space. This space is should be vacuum to ensure the reduction of the heat losses to the surrounding. The losses from the receiver to the glass cover is by radiation. Then, the losses from the receiver to the ambient air is by convection. When the ambient air velocity is small, natural convection dominated. However, when the velocity of the air increased the forced convection effect increase until domination.

Since the purpose of the present work is to reduce the thermal losses from the collector by the trough shape changing, then the problem presented, at first, casually. Consider a parabolic trough facing a wind stream as shown in figure 3.

The trough fixed as shown with the ambient temperature, about 300 ^{o}K. The absorber tube fixed in the middle of the trough with a temperature of 350 ^{o}K, and a diameter of 11.5 cm.

All the properties assumed to be constant, airflow is horizontally with a temperature of 300 ^{o}K, and the absorber surface temperature is uniform at the whole surface. Since the aspect ratio between the troughs diameter to the receiver diameter is very big, then the problem assumed two-dimensional. Regarding combined free and force convection when the ratio of Gr/Red^2 =1, momentum equation will be different and buoyancy should be included as described in **(Bejan. 2004).**

The governing equations for 2-D steady state incompressible fluid flow are time averaged Navir-Stokes equations; RNG-based k-ε turbulent scheme and energy equations as below:

$$\nabla.(\rho U) = 0 (1)$$

$$\rho(U.\nabla)U = \nabla.\left[-PL + (\mu + \mu_T)(\nabla U + (\nabla U)^T) - \frac{2}{3}(\mu + \mu_T)(\nabla.U)l - \frac{2}{3}\rho k_l\right] + F (2)$$

$$\rho(U.\nabla)k = \nabla.\left[\left(\mu + \frac{\mu_T}{\sigma_k}\right)\nabla k\right] + P_k - \rho\epsilon (3)$$

$$\rho(U.\nabla)\epsilon = \nabla.\left[\left(\mu + \frac{\mu_T}{\sigma_e}\right)\nabla\epsilon\right] + C_{e1}\frac{\epsilon}{k}P_k - C_{e2}\rho\frac{\epsilon^2}{k} (4)$$

$$P_k = \mu_T\left[\nabla U : (\nabla U + (\nabla U)^T) - \frac{2}{3}(\nabla.U)^2\right] - \frac{2}{3}\rho k\nabla.U (5)$$

$$\rho C_p U.\nabla T = \nabla.(K\nabla T) + Q + Q_{vh} + W_p (6)$$

$$\mu_T = \rho C_\mu \frac{k^2}{\epsilon} (7)$$

Turbulence model parameters are:

$$C_{e1} \approx 1.44 C_{e2} = 1.92 C_\mu = 0.09$$

$$\sigma_k = 1\sigma_e = 1.30 k_v = 0.41$$

Hydrodynamic boundary conditions for flow analysis are as follows:

- Inlet

  Inlet velocity:

  $$U_o = u (8)$$

  Turbulent intensity:

  $$I_T = \frac{0.16}{(Re_l)^{0.125}} (9)$$

  Turbulence length scale:

$$L_T = 0.07Dh_i (10)$$

Where:

$Re_i = \frac{\rho u Dh_i}{\mu}$ Reynolds number at interring

$Dh_i = \frac{4(9W*\pi W)}{2(9W+\pi W)}$ Hydraulic diameter at interring

- Outlet

Outlet pressure:

$$P_o = 0 (11)$$

$$\left[-PI + (\mu + \mu_T)(\nabla U + (\nabla U)^T) - \frac{2}{3}(\mu + \mu_T)(\nabla . U)I - \frac{2}{3}\rho kI\right] n = -P_o^* n (12)$$

$$P_o^* \leq P_o (13)$$

$$\nabla k . n = 0 (14)$$

$$\nabla \epsilon . n = 0 (15)$$

- Walls

$$\left[(\mu + \mu_T)(\nabla U + (\nabla U)^T) - \frac{2}{3}(\mu + \mu_T)(\nabla . U)I - \frac{2}{3}\rho kI\right] n = -\rho \frac{U_\tau}{\delta_w^+} U_{tang} (16)$$

$$U_{tang} = U - (U.n)n (17)$$

$$U.n = 0 (18)$$

$$\nabla k . n = 0 (19)$$

$$\epsilon = \rho \frac{C_\mu k^2}{k_v \delta_w^+ \mu} (20)$$

- Symmetry wall

$$U.n = 0 (21)$$

$$k = \left[(\mu + \mu_T)(\nabla U + (\nabla U)^T) - \frac{2}{3}\rho kI\right] n (22)$$

$$k - (k.n)n = 0 (23)$$

$$\nabla k.n = 0 (24)$$

$$\nabla \epsilon.n = 0 (25)$$

Thermal boundary conditions on the receiver tube and ambient for flow analysis are as follows:

- Inlet flow temperature:

$$T = T_{amb} = 300\ K (26)$$

- Outlet flow :

$$-n.(-K\nabla T) = 0 (27)$$

- Receiver Tube temperature:

$$T = T_{rt} = 350\ K (28)$$

- Trough wall temperature

$$T = T_{tw} = 300\ K (29)$$

- Symmetry wall

$$-n.(-K\nabla T) = 0 (28)$$

3. DEFINITION OF THE CASE AND NUMERICAL MODEL

The geometry of a full-scale Eurotrough solar collector **(L¨upfert. 2001)** has been selected for this study. Table 1 shows the specification of the Eurotrough solar collector. A typical HCE (heat concentration element) with a stainless steel absorber inner/outer diameter of 6.6/7.0 cm and glass cover of 10.9/11.5 inner/outer diameter has been considered in the simulations. The computational domain is defined by (5W) in the upstream direction, (20W) in the downstream direction, (9 W) in the cross direction and (πW) in the span-wise direction, where W=5.8m is the aperture of the parabola (see the figure 4). The parabolic collector is usually large in length and the aspect ratio of the H CE is very large, thus the flow in span-wise direction can be assumed as spatially periodic.

A uniform wind speed in the inlet velocity profile is considered. Although, the PTCs are exposed to the atmospheric boundary layer, the uniform velocity assumption represents the worst-case scenario for structural loading and could be incorporated as a design safety factor**(Hachicha. 2012)**. Slip conditions are fixed in the top and bottom boundaries, while at the outlet a pressure-based condition is used. At the mirror and HCE surfaces, no-slip conditions are prescribed. As for the span-wise direction, periodic boundary conditions are imposed. The Prandtl number is set to Pr= ν/κ = 0.7 as for air. The temperatures of the glass cover and ambient air are fixed to Trt= 350K and Tamb= 300K, respectively. A Neumann boundary condition ($\partial T/\partial n = 0$) is prescribed in the top, bottom and outlet boundaries for temperature.

The mesh is refined around the collector surface; the HCE near wake and then, stretched going away from the collector (see figures5&6). The mesh is suited for each case of pitch angle and with respect to the dimension of the problem. In order to capture theflow structures in the near wake of the PTC and around the HCE, meshrequirements are higher in these zones. However, due to the large differencebetween the dimensions of the aperture of the parabola and the receiver tube,the construction of the mesh is quite dense and complicated near these elements.The minimum mesh quality is greater than 0.6 and average mesh quality about 0.97 for each pitch angle are presented.In table 2, the main characteristics of the meshes used for each pitch angleare given.

The model treated as non-isothermal flow with turbulent k-ε model. The heat transfer done by forced convection for $\theta = 0^o$, and 90^o, and by mixed free and forced convection for $\theta = 180^o$. The reason behind these assumptions is the value of airflow velocitiesnear the heat transfer region.

The present problem solved by using a finite difference method by using COMSOL Multiphysics v4.4 Program solver. The iterative solution considered to have converged when the maximum of the residual across all nodes is less than 10^{-6} for continuity, velocities, and temperature.

The numerical results checked for grid independency. The procedure repeated whenincreasing the number of nodes until a stage reached where the results produce negligible changes with further refinement in grid size. As it seen in figures 5&6, the meshing refined near the trough collector, and it extra refined near the receiver. The explanation of this meshing is the sever changes in velocities near the collector, and beside of the big change of temperature values near the receiver tube.

4.THE VALIDATION OF THE PRESENT WORK

The aim of the present work is to study the details of flow pattern around a receiver tube, and by combine solution of governing equations, determining thermal losses and convection heat transferring from the receiver tube. Results presented by fluid flow pattern, thermal structure of air around the receiver tube and local Nusselt number around it. Based on the local variation of Nu, average Nu from the glass cover determined and comparison made with the proposed correlations for cross-flow conditions and pure free convection.

Validation of the present numerical scheme obtained by studying the fluid flow over cylinder in two-dimensional as described in **(Hachicha. 2012)**. The computational domain is extended to [−15D, 25D]; [−10D, 10D]; [0, πD] in the stream-, cross- and span-wise directions respectively, and the cylinder with a diameter D is placed at (0, 0, 0). Comparison also made to check the accuracy of thermal field by solving mass, momentum, and energy equation for the cross flow around a horizontal tube. The flow around the cylinder is symmetric and average convection heat transfer computed by the present simulation is the same as Eq.(7.45)**(Incropera. 2011)**, as illustrated in figure 7.

In table3, avalidation done with the numerical data of**Hachicha.2012**. The data checked with previous experimental work.

Table 3 shows the average Nusselt number for the three orientations used in the present work of 0^o, 90^o, and 180^o. The third column shown in the table is the Nusselt number at the front stagnation point. Table 3 also shows the maximum and minimum Nusselt number and the position of that number with degrees.

Table 3 shows a very good agreement with the literatures that proves the accuracy of the present's work procedure.

5. THE RESULTS

After proving the accuracy of the present work, it is confidant now to find the effect of the suggested modification of the shape on the heat transfer process.

Figure 8 below shows the surface temperature distribution on the field for the values of three orientations. The figure shows how the receiver lost its energy to the air passing through it. The

temperature of the air increased due to the direct contact with the tube surface. In the figure 8 (b) it is obvious that the temperature is slightly increased near the edge of the collector due to the increase of the velocity near that edge. This suggests the increase in the air energy.

Figure 8 (c) shows that the receiver high temperature's effect is only on the air near it. The effect dos not spread away due to the fact that the receiver is in the wake of the collector. Therefore, the air velocity near the receiver is very low, where the natural convection dominated and the effect of the buoyant effect appeared.

In figure 9, the effect of the shape modification on the local Nusselt number shown on the receiver with different diameter ratio of 1.3, 1.5, 1.7, and 2. The figures also show the ordinary case of no shape modification. The results show a decrease in the local Nusselt number due to that modification. The astonishing result is the decrease of the overall values especially at the front stagnation point, where the maximum Nusselt number occurs. The fact that the receiver is in the wake of the half-cylindrical disc addedis the only explanation behind that decrement. The half-cylindrical addition cause a decrement of air velocities near the receiver.The values of the local Nusselt number shown to increase to its maximum value at the area just at the end of the disc, where the Nusselt number may increase again due to the facing of the rear part of the receiver to the wake of the flow.

For these cases the addition of the half-cylindrical disc shown to cause a good reduction in the heat transfer losses.

In figure 10, another values shown as in figure 9 above but for the case of 180^o. This case is where the mixed convection appeared. The data shows a slightly reduction in Nusselt number values at the front stagnation point. The reduction increased with arc length of the receiver until reach its maximum value at the back of the receiver.

Figure 11, shows the average Nusselt number with the addition of the half-cylindrical disc for different orientations, and different disc ratio. The figure started with ordinary case with no modification on the shape (the ordinary case). The values show that the maximum heat transfer occurred at 90^o orientation. The data also show how the shape modification causes a decrement in the heat transfer coefficients.

6.CONCLUSIONS

In the present work the heat transfer losses from the receiver to the surrounding with both addition and no addition of a half-cylindrical disc at the front of the receiver. The following points found:

1- At our knowledge, this is the first study of its kind to this case.
2- The addition of the shape modification cause a decrement in the heat transfer coefficient.
3- The maximum decrement occurs at the case of 0^o orientation (i. e. the case of the collector facing the flow).
4- The lowest decrement occurs at 90^o case, which is because the modification of shape works as guides of flow.
5- The increase of the diameter ratio between the half-cylindrical disc and the receiver has a small effect on the heat transfer process.
6- The shape improvement may be a good strategy to decrease the heat losses from the receiver.

7. REFERENCES

1. Al-Ansary, Hany, and Zeitoun, O., "Numerical study of conduction and convection heat losses from a half-insulated air –filled annulus of the receiver of a parabolic trough collector", Solar Energy, 85, pp. 3036-3045, 2011.
2. Bejan A. Convection heat transfer. New York: Wiley; 2004. p. 178–83.
3. Cheng, Z. D., et. al., "Numerical simulation of a parabolic trough collector with nonuniform solar flux conditions by coupling FVM and MCRT method", Solar Energy, 86, pp. 1770-1784, 2012.
4. Cheng, Z. D., et.al, "Three-dimensional numerical study of heat transfer characteristics in the receiver tube of parabolic trough solar collectotr", International Communications in Heat and Mass Transfer, 37, pp. 782-787, 2010.
5. Christ, Farid C., "Numerical modelling of wind and dust patterns around a full-scale paraboloidal solar dish", Renewable Energy, 39, pp. 356-366, 2012.
6. Daniel, Premjit, et. al., "Numerical investigation of parabolic trough receiver performance with outer vacuum shell", Solar Energy, 85, pp. 1910-1914, 2011.
7. Incropera FP, Dewitt DP. Introduction to heat transfer, sixth edition. John Wiley & Sons, Inc; 2011.
8. Kalogirou, Soteris A., "A detailed thermal model of a parabolic trough collector receiver", Energy, 48, pp. 298-306, 2012.
9. L¨upfert E, Geyer M, Schiel W, Esteban A, Osuna R, Zarza E, et al. EUROTROUGH design issues and prototype testing at PSA. In: Proceedings of ASME International Solar Energy Conference- Forum 2001. Washington, DC: Solar Energy: The power to Choose; April 21-25, p. 289–394.
10. Hachicha, A. A., et.al."Numerical simulation of wind flow around a parabolic trough solar collector", Print submitted to Applied Energy, November 20, 2012.
11. Naeeni, M., and Yaghoubi, M., "Analysis of wind flow around a parabolic collector (2) heat transfer from receiver tube", Renewable Energy, 32, pp. 1259-1272, 2007.
12. Naeeni N, Yaghoubi M. Analysis of wind flow around a parabolic collector (1) Fluid flow. Renewable Energy An Int J, submitted for publication.
13. Padilla, Ricardo Vasquez, et. al., "Heat transfer analysis of parabolic trough solar receiver", Applied Energy, 88, pp. 5097-5110, 2011.

Table-1: The specification of the Euro trough solar collector (L¨upfert.2001)

Layout	**parabolic trough collector**
Support structure	steel frame work, pre-galvanized, two variants with light weight, low torsion
Collector length	12 m per element; 100 - 150 m collector length
Drive	hydraulic drive
Max. wind speed	operation: 14 m/s; stow: 40 m/s
Tracking control	Mathematical algorithm + angular encoder checked by sun sensor
Parabola	$y = x^2/4f$ with f = 1.71 m
Aperture width (W)	5.8 m
Reflector	28 glass facets per SCE
Absorber tube	evacuated glass envelope, UVAC® or other, application dependent
Fluid	oil, steam, application dependent
Cost	< 200 Euro/m^2

Table 2: Details of adopted meshes for each pitch angle

Pitch angle	0^o	90^o	180^o
Number of element	90929	45765	31256
Minimum mesh quality	0.6376	0.6111	0.6475
Average mesh quality	0.9703	0.9724	0.97

Tabe 3 The validation datas.

	Position	Nua	Nu_{fsp}	Nu_{max}/Pos	Nu_{min}/Pos
Hachicha [4]	0^o	24.5	33.1	41.4/289.5^o	9.5/196.8^o
Present work	0^o	25.8	32.79	34.38/313.7^o	10.9/132.5^o
Hachicha [4]	90^o	47.4	86	86/0^o	27.3/222^o
Present work	9^o	48.3	67.7	69.8/22^o	19.99/204.8^o
Hachicha [4]	180^o	22.5	23.7	29.1/269.5^o	7.4/85.9^o
Present work	180^o	21.66	19.1	25.82/188.8^o	15.64/56.3^o
Hachicha [4]	Cylinder in cross flow	52.2	86	86.57/357.4^o	17.4/272.2^o
Present work	Cylinder in cross flow	47.4	45.37	45.37/360^o	17.16/207.9^o

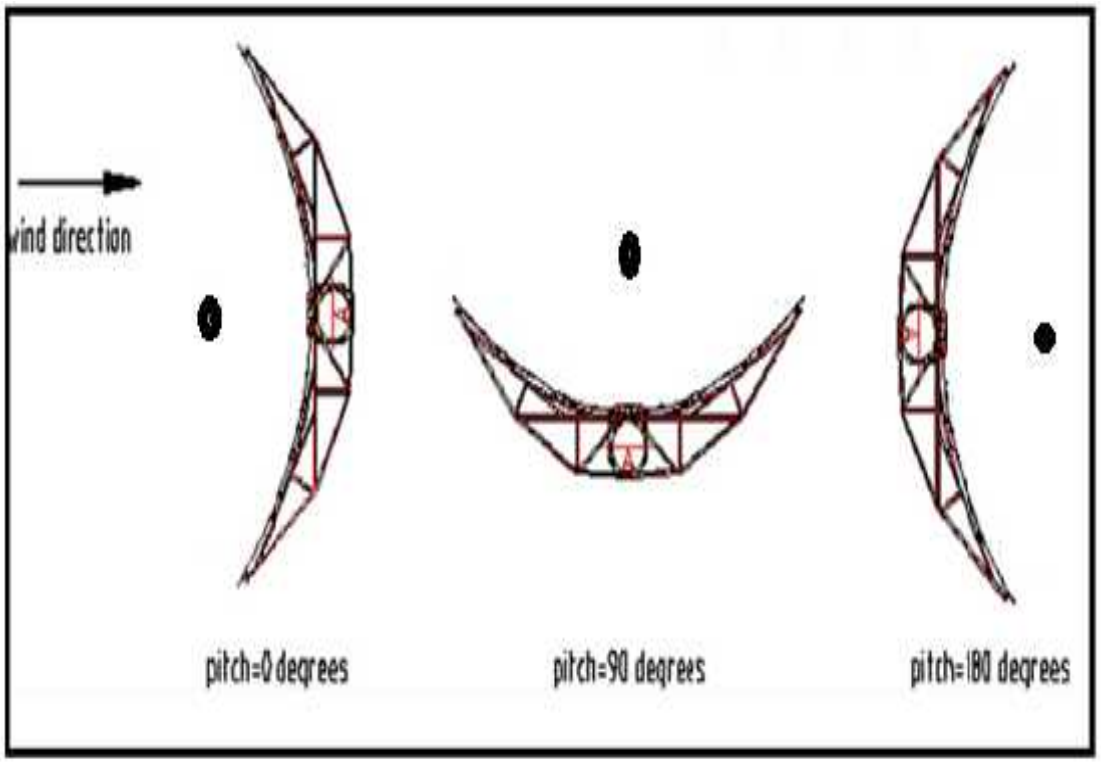

Figure 1: The orientations of the present work.

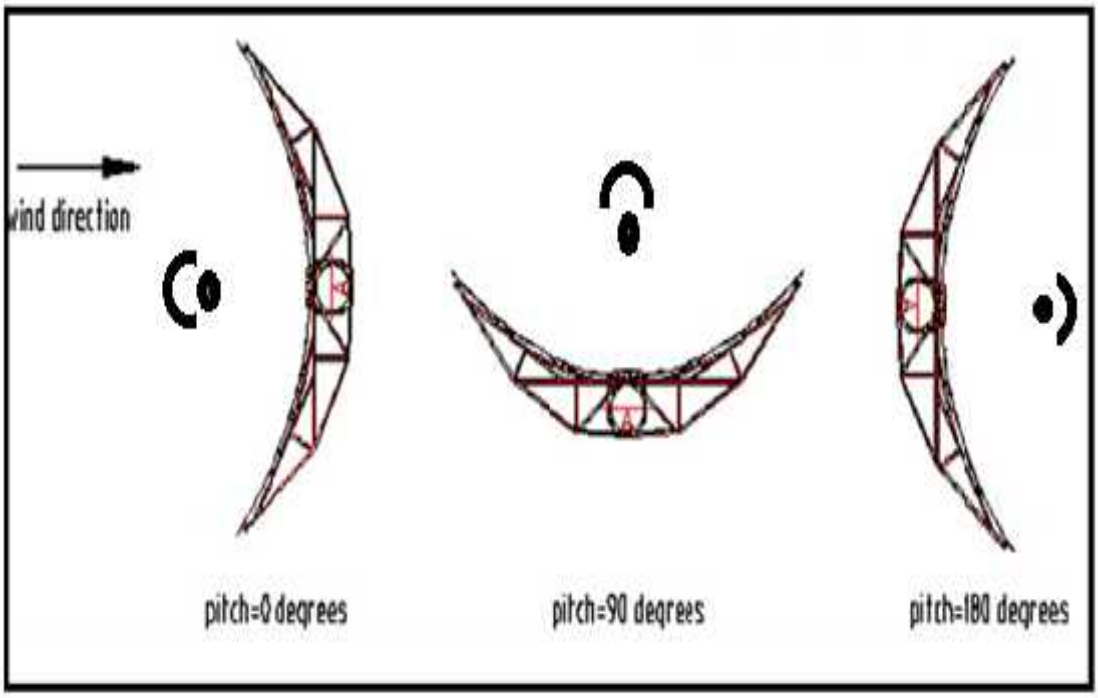

Figure 2: The suggested modification in the present work.

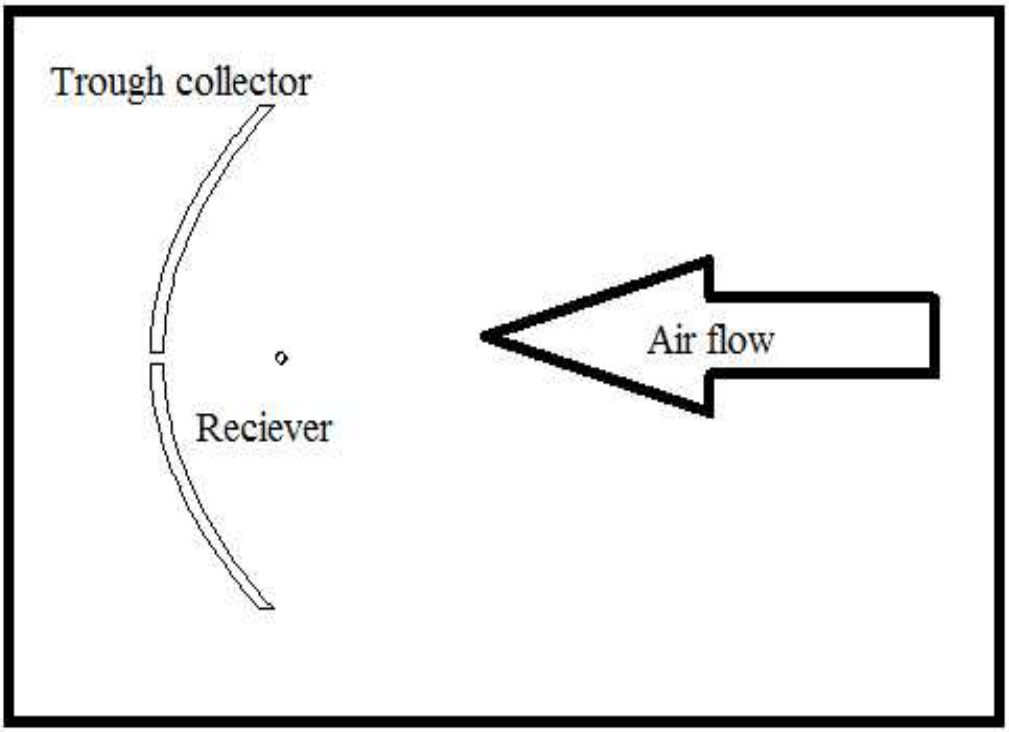

Figure 3 The trough collector case study.

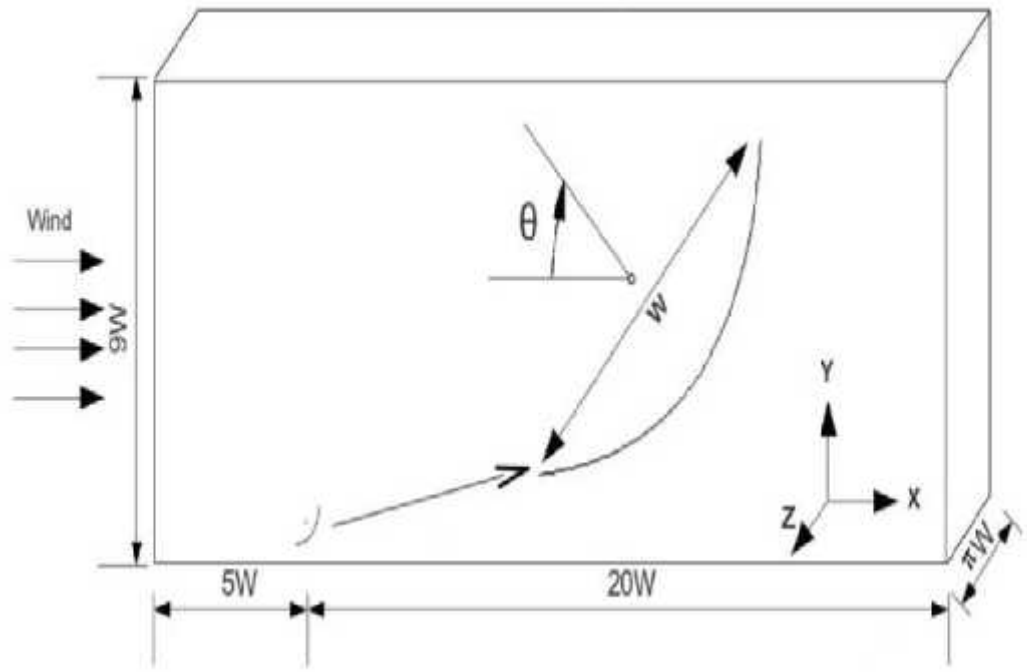

Figure 4: Computational domain of the wind flow study around an Euro trough solar collector [Hachicha. 2012].

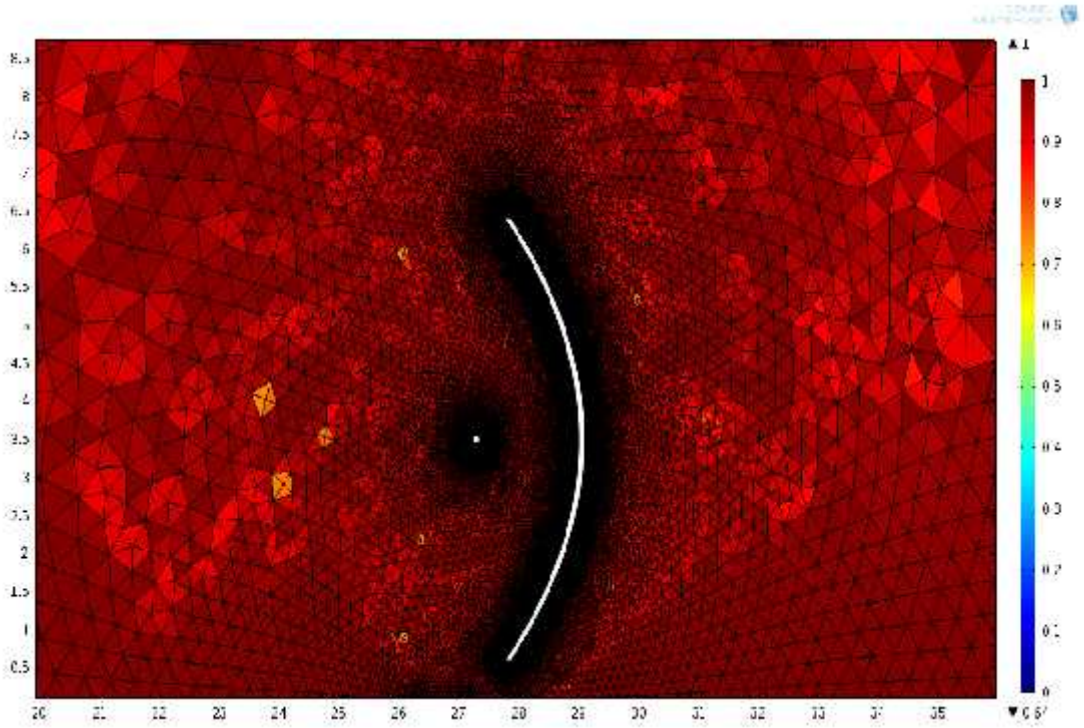

Figure 5: Mesh Quality around the mirror and HCE

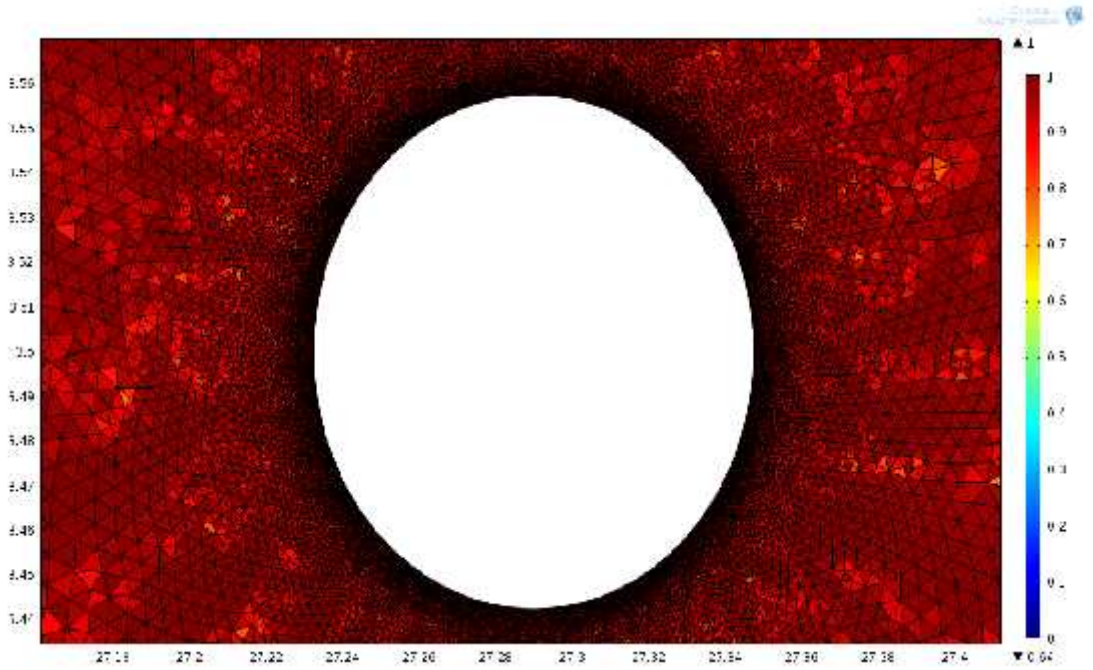

Figure 6: Mesh quality around the HCE (Heat Concentration Element)

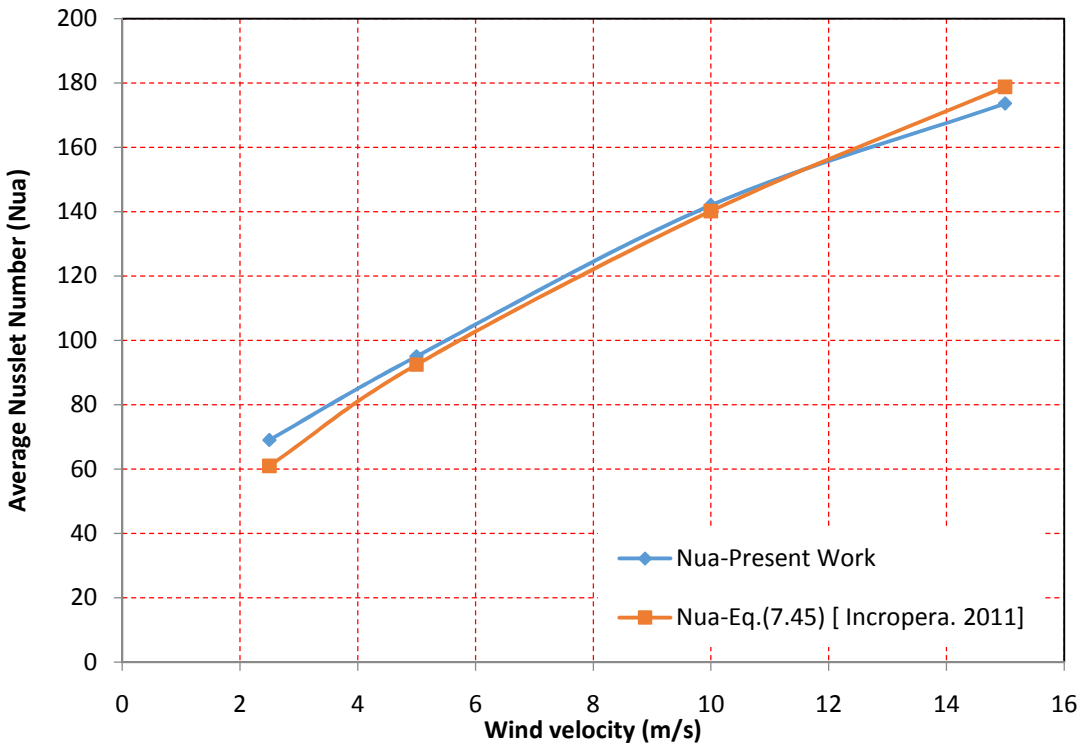

Figure 7: Variation of average Nusselt number and wind speed

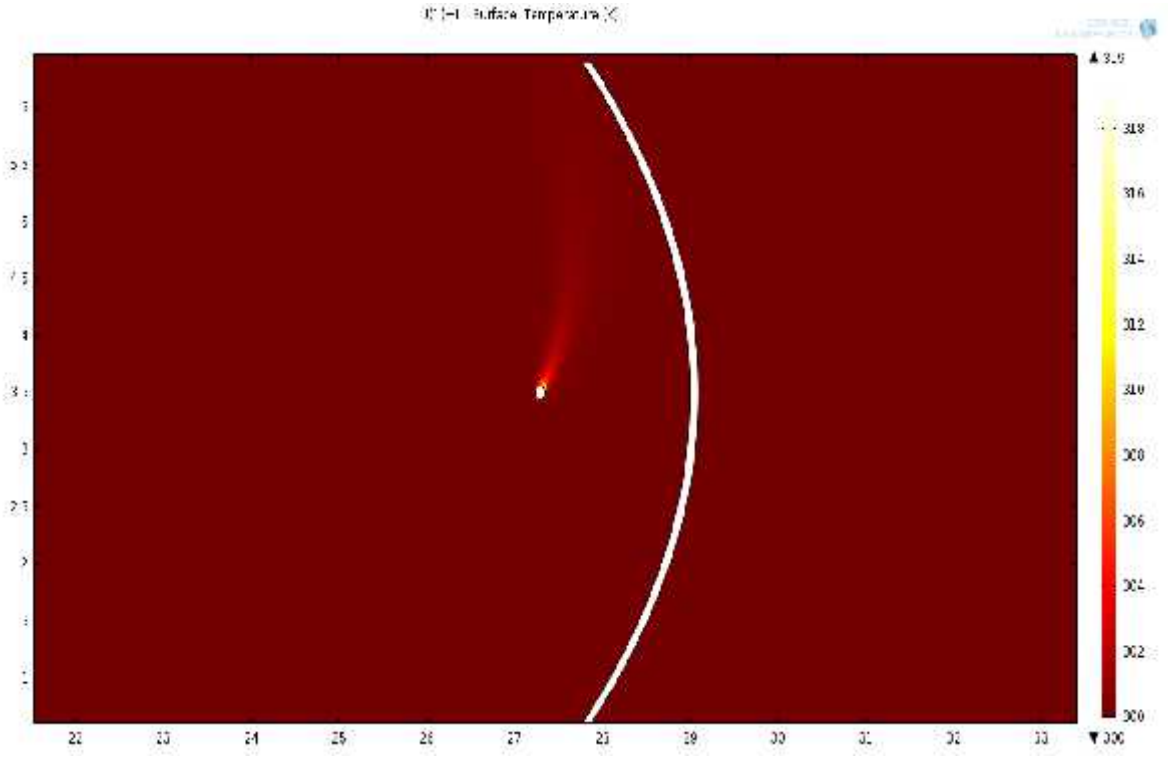

(a)

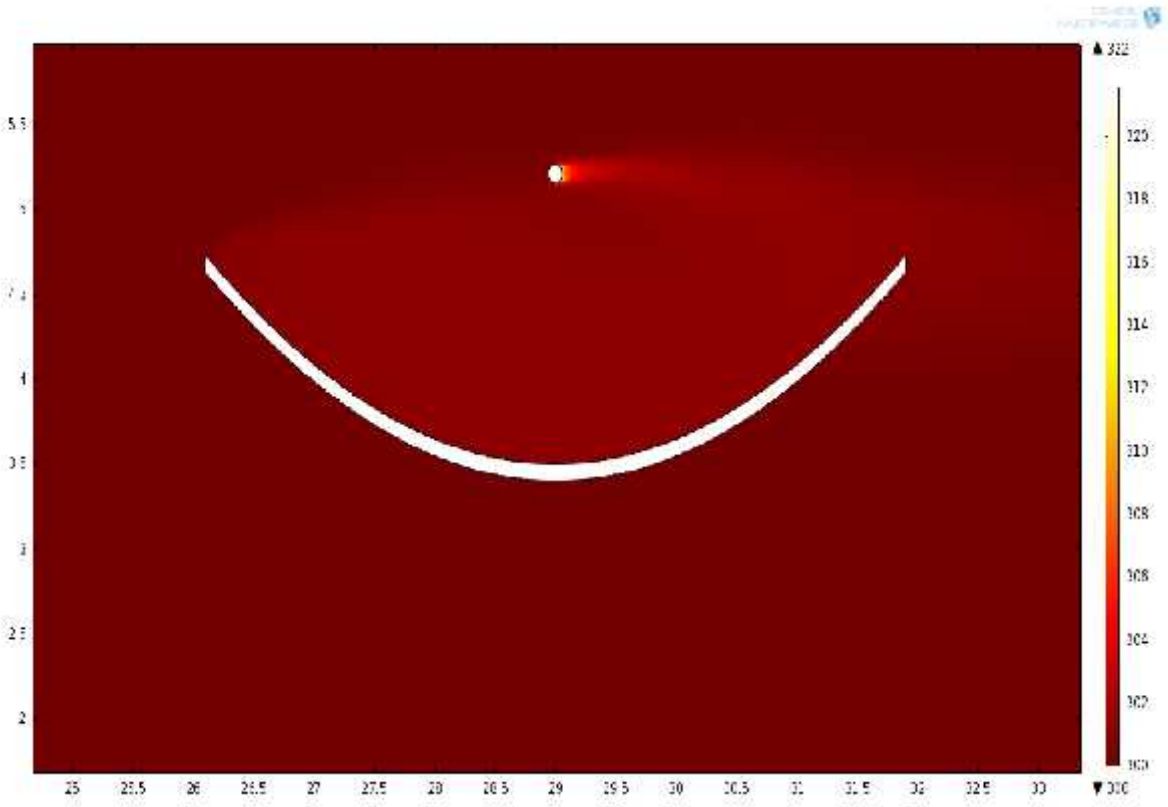

(b)

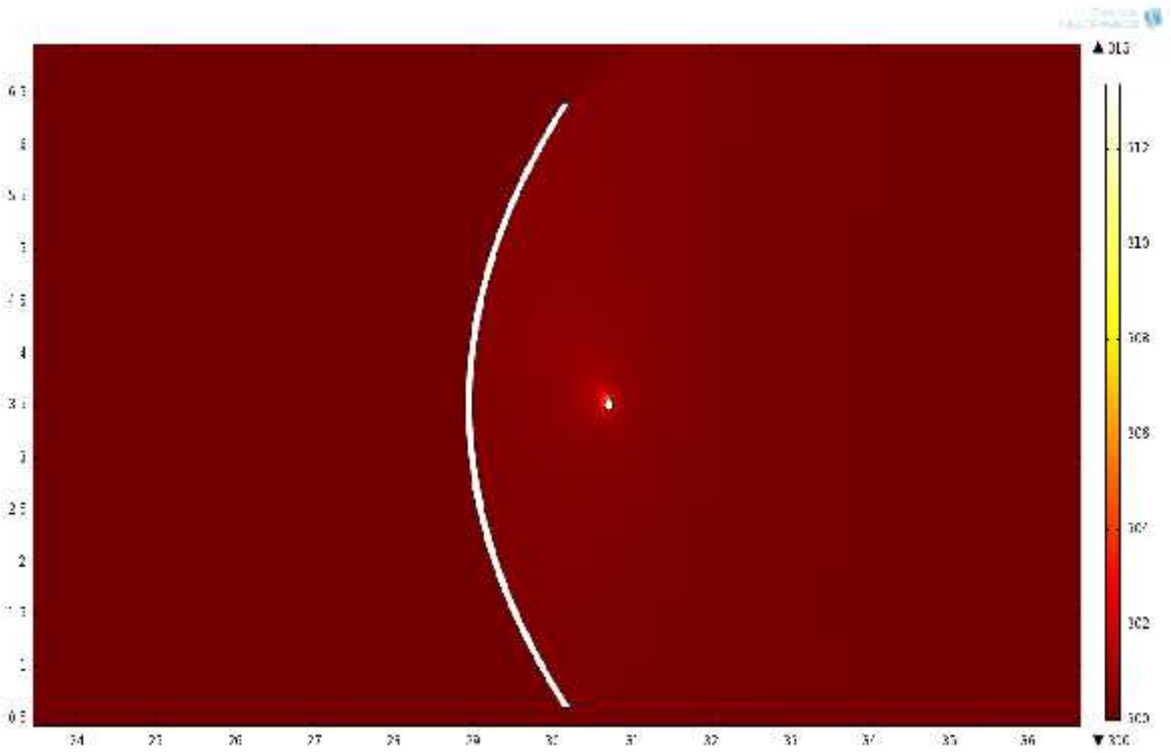

(c)

Figure 8 Temperature distribution around the PTC for different pitch angles: (a) θ=0^o, (b) θ=90^o, (c) θ=180^o

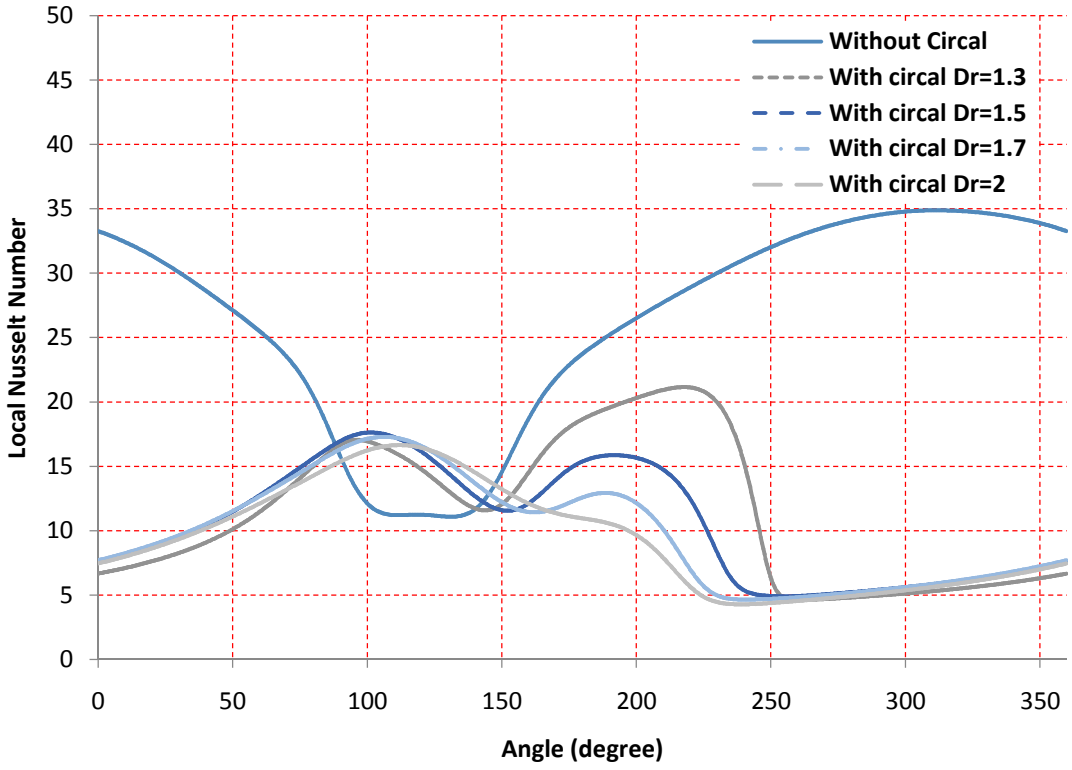

(a)

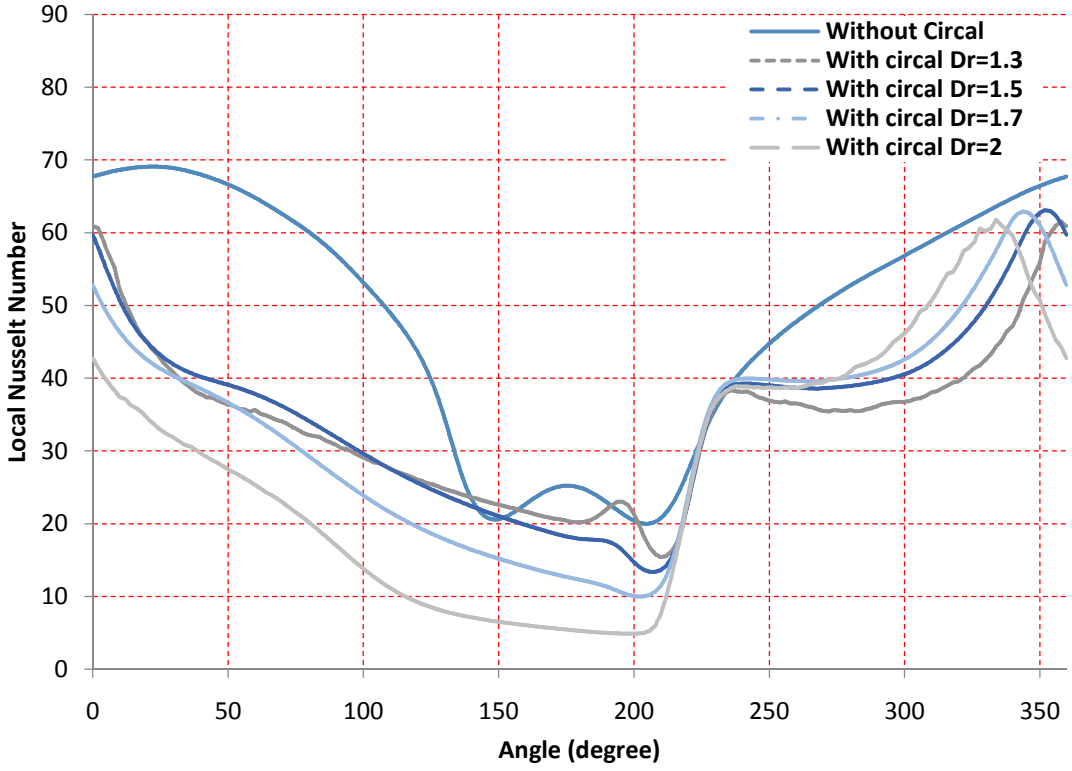

(b)

Figure 9 Variation of the local Nusselt number around the HCE for different pitch angles: (a) θ=0^o, (b) θ=90^o forced convection

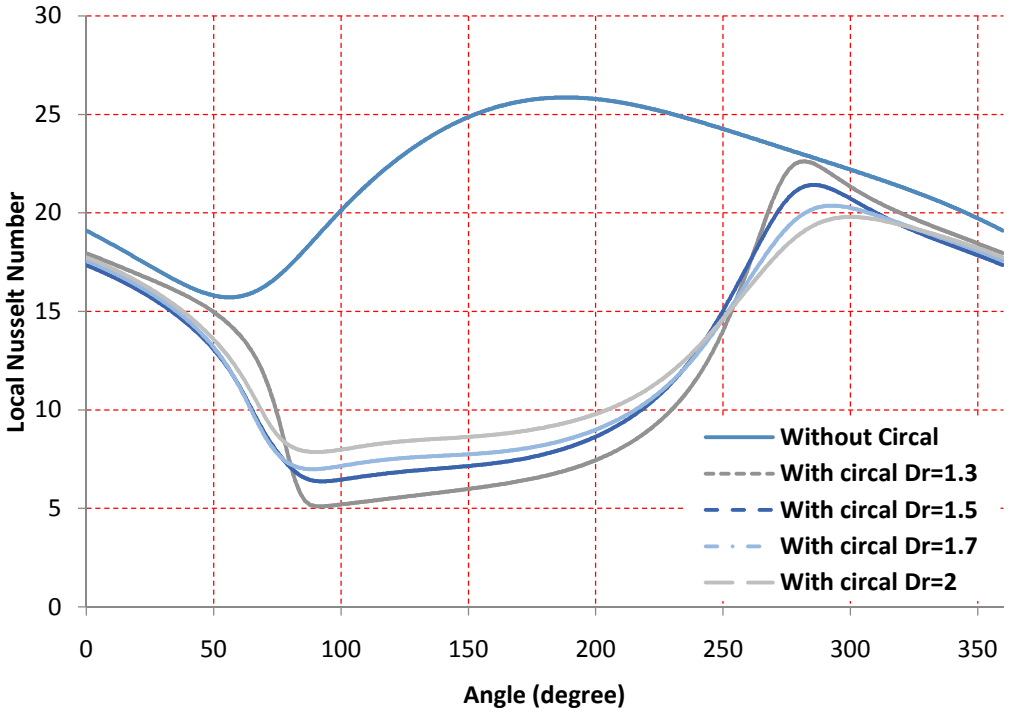

Figure 10 Variation of the local Nusselt number around the HCE for pitch angles: (θ=180^o) mixed convection.

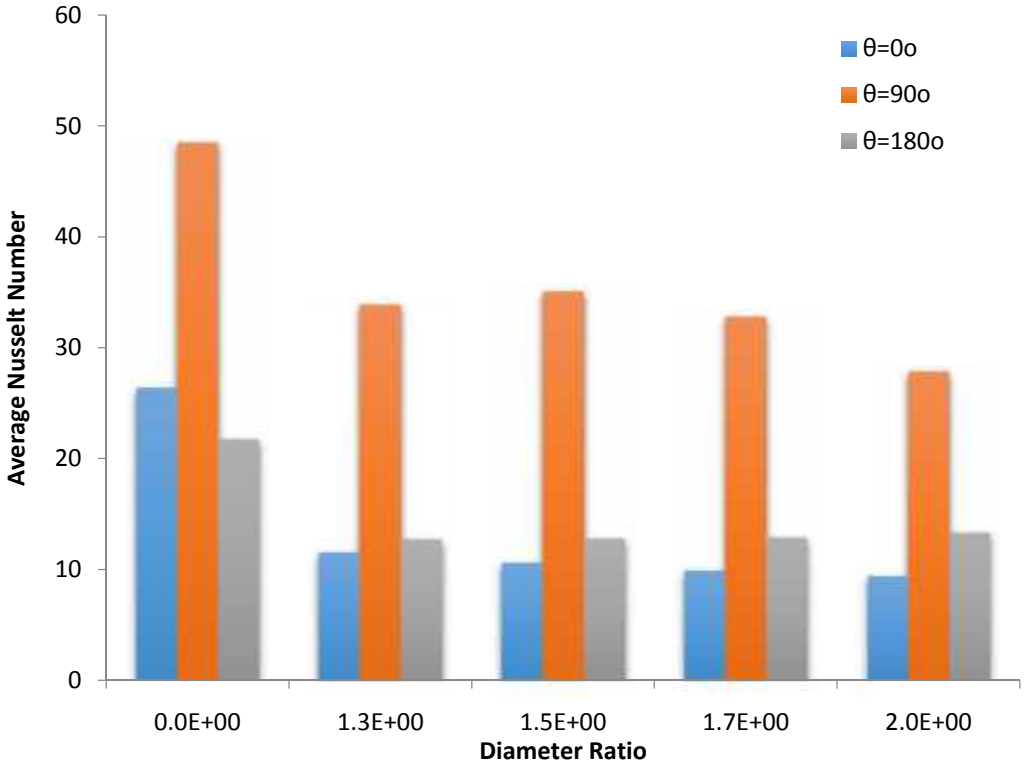

Figure 11 Variation of the average Nusselt number around the HCE with diameter ratio (Dr).